

# Constructal design of Y-shaped assembly of fins

Giulio Lorenzini <sup>a,\*</sup>, Luiz Alberto Oliveira Rocha <sup>b</sup>

<sup>a</sup> *Department of Agricultural Economics and Engineering, Alma Mater Studiorum-University of Bologna, viale Giuseppe Fanin no. 50, 40127 Bologna, Italy*

<sup>b</sup> *Departamento de Física, Fundação Universidade Federal do Rio Grande, Cx.P. 474, Rio Grande, RS 96201-900, Brazil*

Received 10 February 2006

Available online 25 July 2006

## Abstract

This work relies on constructal design to perform the geometric optimization of the Y-shaped assembly of fins. It is shown numerically that the global thermal resistance of the Y-shaped assembly of fins can be minimized by geometric optimization subject to total volume and fin material constraints. A triple optimization showed the emergence of an optimal architecture that minimizes the global thermal resistance: an optimal external shape for the assembly, an internal optimal ratio of plate-fin thicknesses and an optimal angle between the tributary branches and the horizontal. Parametric study was performed to show the behavior of the minimized global thermal resistance. The results also show that the optimized Y-shaped structure performs better than the optimized T-shaped one.

© 2006 Elsevier Ltd. All rights reserved.

*Keywords:* Constructal theory; Enhanced heat transfer; Fins; Optimization

## 1. Introduction

Constructal design has been applied to a large variety of engineering problems, e.g., [1–4], to optimize shape and structure [5]. On the other hand, the augmentation of heat transfer has been pursued for a long time in the engineering field. Individual fins and assemblies of fins have been studied exhaustively and the results can be found in some reviews [6,7]. Recently, constructal design has been applied successfully to the geometrical optimization of fins. Bonjour et al. [8] documents the fundamental relation between the maximization of global performance and the malleable (morphing) architecture in the coaxial two-stream heat exchanger. Configurations with radial and branched fins were optimized. Vargas et al. [9] conducted a combined numerical and experimental study to maximize heat transfer by optimizing a finned circular and elliptic tubes heat exchangers.

Constructal design has also been used in the study of cavities, i.e., inverted or negative fins. Biserni et al. [10] optimized C- and T-shaped cavities while Rocha et al. [11] optimized the trapezoidal external shape of C-shaped cavities. Both of the works minimized the global thermal resistance while the total volume and the cavity volume were kept as constraints. Bejan and Almgöbel [12] optimized several types of assembly of fins that have been recognized in practice including the T-shaped assembly of fins. The objective of the T-shaped constructal optimization was to maximize the global thermal conductance of the assembly subject to total volume and fin-material constraints. The two degrees of freedom of the T-shaped structure were the external shape and the internal ratio of plate-fin thickness for the assembly.

This work relies on the constructal design to optimize the complete geometry of the Y-shaped assembly of fins, i.e., the T-shaped structure version with an additional degree of freedom: the angle between a tributary branch and the horizontal. The objective is to minimize the global thermal resistance subject to the total volume and fin-material constraints.

\* Corresponding author. Tel.: +39 051 2096186; fax: +39 051 2096178.  
E-mail addresses: [giulio.lorenzini@unibo.it](mailto:giulio.lorenzini@unibo.it) (G. Lorenzini), [dfsrocha@furg.br](mailto:dfsrocha@furg.br) (L.A. Oliveira Rocha).

### Nomenclature

$a$	dimensionless parameter, Eq. (9)
$A$	area [ $\text{m}^2$ ]
$h$	heat transfer coefficient [ $\text{W m}^{-2} \text{K}^{-1}$ ]
$k$	fin thermal conductivity [ $\text{W m}^{-1} \text{K}^{-1}$ ]
$L$	length [m]
$q$	heat current [W]
$t$	thickness [m]
$T$	temperature [K]
$V$	volume [ $\text{m}^3$ ]
$W$	width [m]

### Greek symbols

$\alpha$	angle between the tributary branches and the horizontal
----------	---

$\theta$	dimensionless temperature, Eq. (5)
$\phi$	volume fraction of fin material

### Subscripts

f	fin material
m	single optimization
mm	double optimization
mmm	triple optimization

### Superscript

( )	dimensionless variables, Eqs. (6), (7), (10), (11), (14) and (15)
-----	---

## 2. Mathematical model

Consider the Y-shaped assembly of fins sketched in Fig. 1. Two elemental fins of thickness  $t_0$  and length  $L_0$  serve as tributaries to a stem of thickness  $t_1$  and length  $L_1$ . The elemental fin of thickness  $t_0$  forms an angle  $\alpha$  with a horizontal line. The configuration is two-dimensional, with the third dimension ( $W$ ) sufficiently long in comparison with  $L_0$  and  $L_1$ . The heat transfer coefficient  $h$  is uniform over all the exposed surfaces. The heat current through the root section ( $q_1$ ) and the temperature of the fluid ( $T_\infty$ ) are known. The maximum temperature ( $T_{1,\max}$ ) occurs at the root section ( $y=0$ ) and varies with the geometry.

The objective of the analysis is to determine the optimal geometry ( $L_1/L_0, t_1/t_0, \alpha$ ) that is characterized by the minimum global thermal resistance  $(T_{1,\max} - T_\infty)/q_1$ . According to constructal design [5], this optimization is subjected to two constraints, namely, the total volume (i.e., frontal area) constraint,

$$A = (L_1 + L_0 \sin \alpha + t_0 \cos \alpha)(2L_0 \cos \alpha + t_1) \quad (1)$$

and the fin-material volume constraint,

$$A_f = L_1 t_1 + 2L_0 t_0 + t_1 t_0 \cos \alpha - t_0^2 \sin \alpha \cos \alpha \quad (2)$$

The latter can be expressed as the fin volume fraction

$$\phi = A_f/A \quad (3)$$

The analysis that delivers the global thermal resistance as a function of the assembly geometry consists of solving numerically the heat conduction equation along the Y-shaped assembly of fins where the fins are considered isotropic with constant thermal conductivity  $k$

$$\frac{\partial^2 \theta}{\partial \tilde{x}^2} + \frac{\partial^2 \theta}{\partial \tilde{y}^2} = 0 \quad (4)$$

where the dimensionless variables are

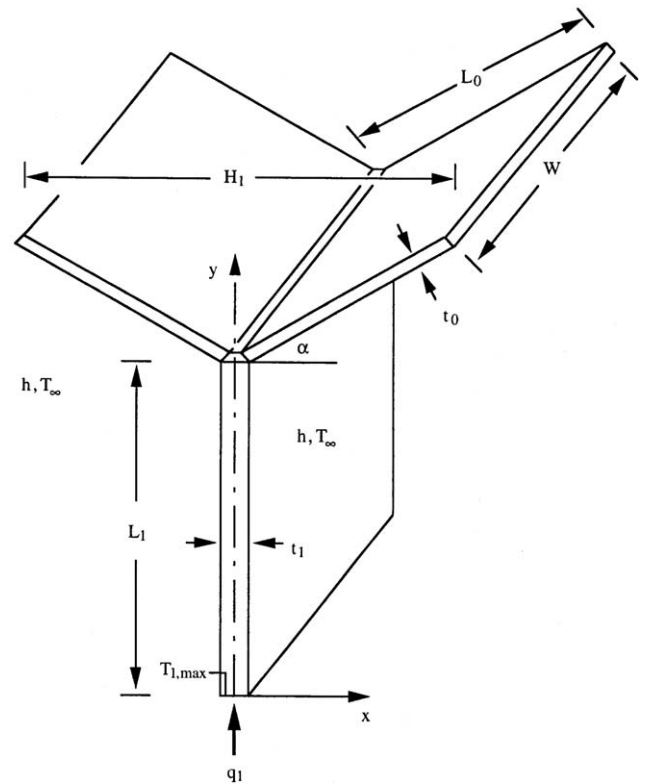


Fig. 1. Y-shaped assembly of fins analyzed.

$$\theta = \frac{T - T_\infty}{q_1/kW} \quad (5)$$

and

$$\tilde{x}, \tilde{y}, \tilde{t}_0, \tilde{L}_0, \tilde{t}_1, \tilde{L}_1 = \frac{x, y, t_0, L_0, t_1, L_1}{A^{1/2}} \quad (6)$$

The boundary conditions are given by

$$-\frac{\partial \theta}{\partial \tilde{y}} = \frac{1}{t_1} \quad \text{at } \tilde{y} = 0 \quad (7)$$

and

$$-\frac{\partial\theta}{\partial\tilde{y}} = \frac{a^2}{2}\theta \quad \text{or} \quad -\frac{\partial\theta}{\partial\tilde{x}} = \frac{a^2}{2}\theta \quad \text{at the other surfaces} \quad (8)$$

The parameter ( $a$ ) that emerged in Eq. (8) was already used by Bejan and Almgöbel [12] and defined as

$$a = \left(\frac{2hA^{1/2}}{k}\right)^{1/2} \quad (9)$$

The dimensionless form of Eqs. (1) and (3) are

$$1 = (\tilde{L}_1 + \tilde{L}_0 \sin \alpha + \tilde{t}_0 \cos \alpha)(2\tilde{L}_0 \cos \alpha + \tilde{t}_1) \quad (10)$$

$$\phi = \frac{A_0}{A} = \tilde{L}_1 \tilde{t}_1 + 2\tilde{L}_0 \tilde{t}_0 + \tilde{t}_1 \tilde{t}_0 \cos \alpha - \tilde{t}_0^2 \sin \alpha \cos \alpha \quad (11)$$

The maximal excess temperature,  $\theta_{1,\max}$ , is also the dimensionless global thermal resistance of the construct,

$$\theta_{1,\max} = \frac{T_{1,\max} - T_\infty}{q_1/kW} \quad (12)$$

### 3. Numerical model

The function defined by Eq. (12) can be determined numerically, by solving Eq. (4) for the temperature field in every assumed configuration ( $L_1/L_0, t_1/t_0, \alpha$ ), and calculating  $\theta_{1,\max}$  to see whether  $\theta_{1,\max}$  can be minimized by varying the configuration. In this sense, Eq. (4) was solved using a finite elements code, based on triangular elements, developed in MATLAB environment, precisely the PDE (partial-differential-equations) toolbox [13]. The grid was non-uniform in both  $\tilde{x}$  and  $\tilde{y}$ , and varied from one geometry to the next. The appropriate mesh size was determined by successive refinements, increasing the number of elements four times from the current mesh size to the next mesh size, until the criterion  $|(\theta_{i,\max}^j - \theta_{i,\max}^{j+1})/\theta_{i,\max}^j| < 2 \times 10^{-4}$  was satisfied. Here  $\theta_{i,\max}^j$  represents the maximum temperature calculated using the current mesh size, and  $\theta_{i,\max}^{j+1}$  corresponds to the maximum temperature using the next mesh, where the number of elements was increased by four times. Table 1 gives an example of how grid independence was achieved. The following results were performed by using a range between 2000 and 10,000 triangular elements.

To test the accuracy of the numerical code, the numerical results obtained using our code in Matlab PDE have been compared with the analytical results obtained by Bejan and Almgöbel [12]. The domain in this case was a

Table 1  
Numerical tests showing the achievement of grid independence ( $\phi = 0.1, a = 0.1, t_1/t_0 = 4, L_1/L_0 = 0.1, \alpha = 1.47$ )

Number of elements	$\theta_{1,\max}^j$	$ (\theta_{1,\max}^j - \theta_{1,\max}^{j+1})/\theta_{1,\max}^j $
132	38.3513	$9.569 \times 10^{-4}$
528	38.3880	$3.543 \times 10^{-4}$
2112	38.4016	$1.276 \times 10^{-4}$
8448	38.4065	

Table 2

Comparison between the results obtained using our MATLAB partial-differential-equations (PDE) toolbox code and the analytical results [2] ( $\phi = 0.2, a = 0.1$ )

	$L_1/L_0$	$t_1/t_0$	$(\theta_{1,\max})_{\text{mm}}$
Analytical	0.07	4.0	0.033
Numerical	0.071	4.0	0.0332

T-shaped assembly of fins ( $\alpha = 0$ ). Table 2 shows that the two sets of results agree very well. The label “mm” for the minimal global thermal resistance in Table 2 means that it was minimized twice, i.e., with respect to the ratios  $L_1/L_0$  and  $t_1/t_0$ .

### 4. Optimal Y-shaped geometry

The numerical work consisted of determining the temperature field in a large number of configurations of the type shown in Fig. 1. Fig. 2 shows that there is an optimal angle ( $\alpha = 1.47 = 84.2^\circ$ ) that minimizes the global thermal resistance when the parameters ( $\phi, a$ ) and the degrees of freedom ( $L_1/L_0, t_1/t_0$ ) are fixed. The best shape calculated is also drawn in scale in Fig. 2, therefore it can illustrate this optimal Y-shaped assembly of fins.

The procedure used to obtain the best angle in Fig. 2 is now repeated fixing the  $L_1/L_0$  degree of freedom and varying the ratio  $t_1/t_0$ . The minimal global thermal resistance calculated in each case is labeled “m” and the corresponding optimal angle receives the label “o”. The minimal global thermal resistance,  $(\theta_{1,\max})_m$ , and the corresponding optimal angle,  $\alpha_o$ , are plotted in Fig. 3. This figure shows that there is an optimal ratio  $t_1/t_0$  that minimizes the global thermal resistance when the ratio  $L_1/L_0$  is fixed. However, these changes in the value of  $(\theta_{1,\max})_m$  with respect to  $t_1/t_0$  are so small that we conclude that  $t_1/t_0$  is not a critical degree of freedom in the present optimization. On the other

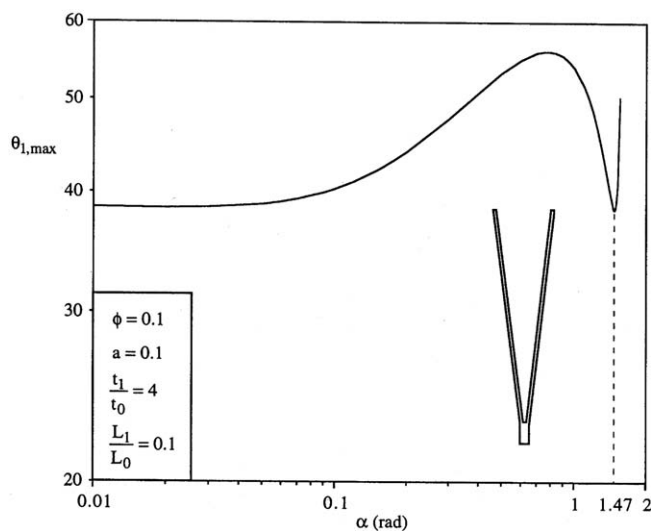


Fig. 2. Optimal angle that minimizes the global thermal resistance for fixed parameters and degrees of freedom.

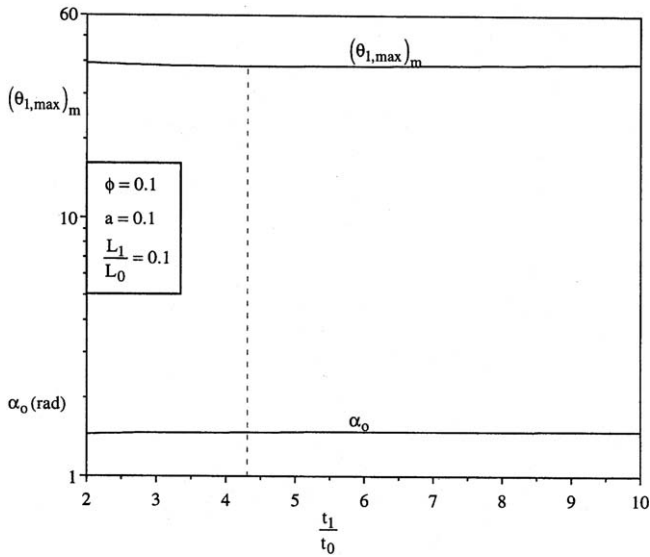


Fig. 3. Second opportunity of optimization.

hand, it shows that the optimal angle,  $\alpha_o$ , increases very little when the ratio  $t_1/t_0$  increases.

Fig. 3 also demonstrates that there is a second opportunity of optimization. Therefore, the procedure used in Fig. 3 was repeated for several  $L_1/L_0$  ratios. The results were summarized in Fig. 4. This figure shows that the global thermal resistance now minimized twice,  $(\theta_{1,max})_{mm}$ , decreases monotonically as the ratio  $L_1/L_0$  decreases. The now double optimized optimal angle,  $\alpha_{oo}$ , also decreases monotonically as the ratio  $L_1/L_0$  increases, but these changes can be more easily noted for large values of  $L_1/L_0$ . It is interesting to note that the optimal  $\alpha$  shown in Figs. 3 and 4 does not depend on changes in the ratios  $L_1/L_0$  and  $t_1/t_0$ , i.e., it appears to be insensitive to changes in these ratios.

The optimal ratio  $(t_1/t_0)_o$  is also shown in Fig. 4. According to Fig. 4, the best Y-shaped assembly of fins,

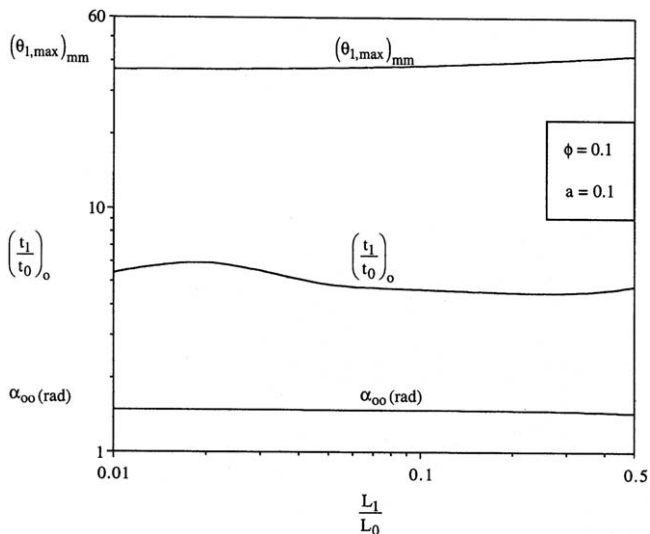


Fig. 4. General results of the optimization.

i.e., the triple optimized thermal resistance is found when  $L_1/L_0$  tends to zero ( $L_1/L_0 = 0.01$ ) and the parameters  $\phi = 0.1$  and  $a = 0.1$  are used. The procedure used for the triple optimization is now repeated for several values of  $\phi$  in Fig. 5. This figure shows that the three times minimized thermal resistance,  $(\theta_{1,max})_{mmm}$ , decreases monotonically while the three times optimized angle  $\alpha, \alpha_{ooo}$ , increases monotonically when  $\phi$  increases. We can also observe that the twice-optimized ratio  $(t_1/t_0)_{oo}$  almost does not depend on  $\phi$  and can be considered approximately constant and equal to 6.

The triple optimization shown in Figs. 2–4 is repeated as function of the parameters  $(\phi, a)$ . The range  $0.05 \leq a \leq 0.2$  was chosen following Bejan and Almgobel [12] where they suggest  $a = 10^{-1}$  as a good value in forced convection to gas flow. Kraus [6] also presents a numerical example using  $a = 0.185$ . These results are presented in Figs. 6–9. Fig. 6 shows that  $(\theta_{1,max})_{mmm}$  decreases monotonically as  $\phi$  and  $a$  increases. Fig. 7 shows that the triple optimized  $\alpha$  angle,

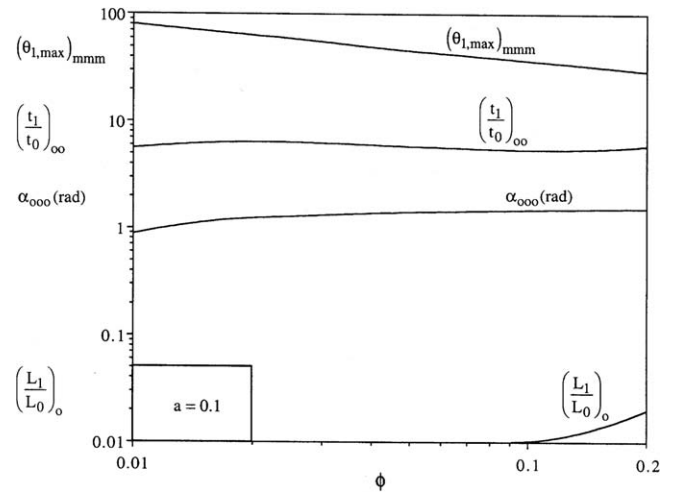


Fig. 5. Triple optimization repeated for several values of  $\phi$ .

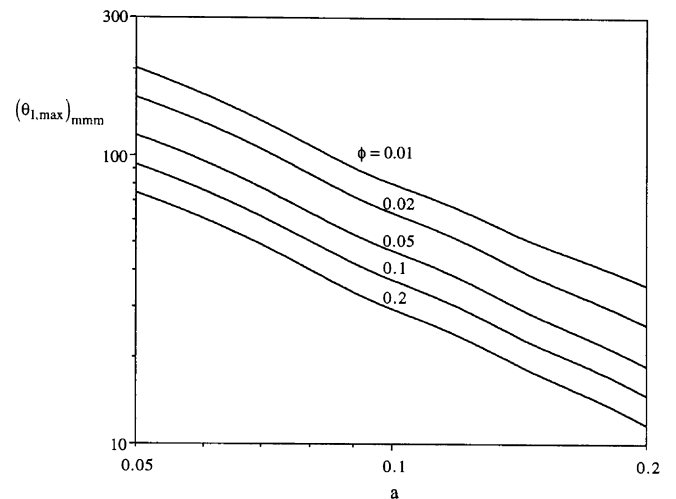


Fig. 6. Trend of the three times minimized thermal resistance with  $\phi$  and  $a$ .

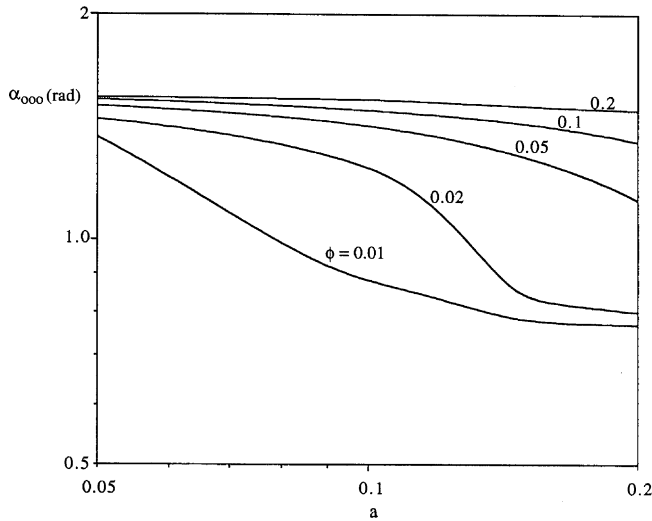


Fig. 7. Trend of the three times minimized angle  $\alpha$  with  $\phi$  and  $a$ .

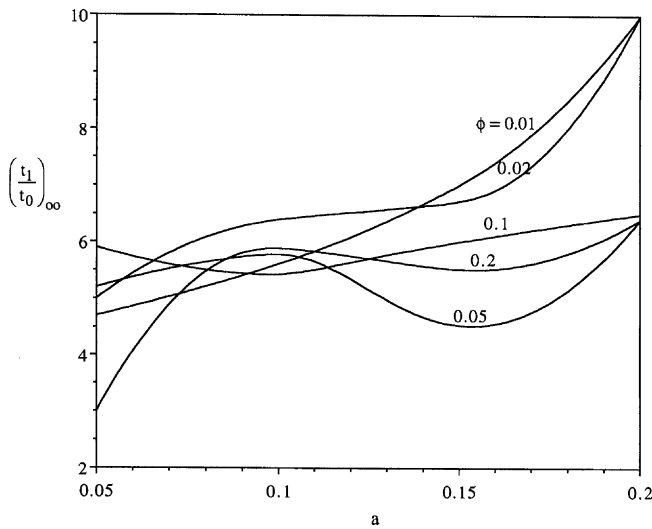


Fig. 8. Trend of the twice-optimized ratio  $(t_1/t_0)_{oo}$  with  $\phi$  and  $a$ .

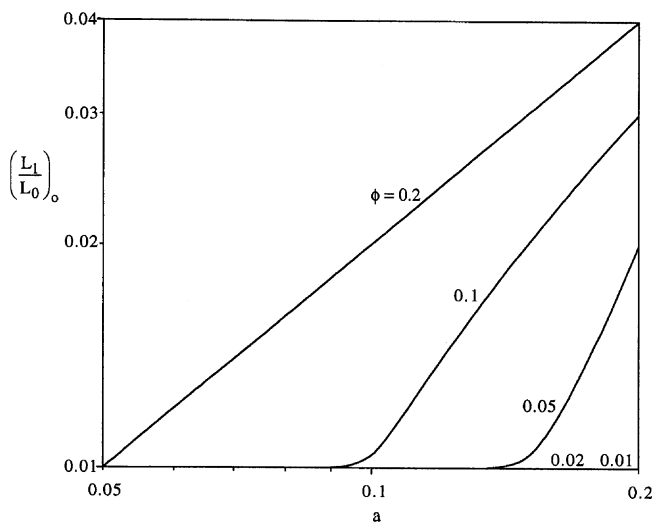


Fig. 9. Trend of the optimized ratio  $(\frac{L_1}{L_0})_o$  with  $\phi$ .

$\alpha_{ooo}$ , increases when the  $\phi$  value increases and the ( $a$ ) parameter decreases. In the range  $0.05 \leq a \leq 0.2$ ,  $0.01 \leq \phi \leq 0.2$  and  $0.78 \leq \alpha \leq 1.55$  the results shown in Figs. 6 and 7 are correlated within 8.3% by the power law

$$(\theta_{1,max})_{mmm} = 0.82a^{-1.33} \phi^{-0.33} \alpha_{ooo}^{-0.07} \quad (13)$$

The twice-optimized ratio  $(t_1/t_0)_{oo}$  has a different behavior than the one presented by the former figures and its values are shown in Fig. 8 as function of the parameters ( $\phi, a$ ).

Finally, Fig. 9 shows that the optimized ratio  $(\frac{L_1}{L_0})_o$  increases with the value of  $\phi$  and  $a$  and it is approximately zero for small values of  $\phi$  in the range studied.

### 5. Comparison of the performance and optimal geometry between the Y- and T-shaped fins

The domain shown in Fig. 1 assumes a T-shaped assembly of fins when the angle  $\alpha$  is equal to zero. The T-shaped mathematical model is the same used in Section 2, except by Eqs. (10) and (11) which are replaced by the equations below,

$$2\tilde{L}_0\tilde{L}_1 = 1 \quad (14)$$

and

$$\phi = 2\tilde{L}_0\tilde{t}_0 + \tilde{L}_1\tilde{t}_1 \quad (15)$$

In this section we compare the results we got for our Y-shaped assembly of fins with the ones obtained by the T-shaped fins model. The numerical method, mesh refinement and accuracy tests are the same used in Section 3. Fig. 10 shows that the optimized thermal resistance obtained for the Y-shaped fins is smaller than that obtained for the T-shaped fins. This better performance increases with the value of the parameter ( $a$ ) and it is approximately 11% when  $a = 0.2$ . The optimal ratio  $(t_1/t_0)_{oo}$  values are approximately 12% larger in the Y-shaped fins case than the values of the T-shaped fins case. Fig. 10 also shows that

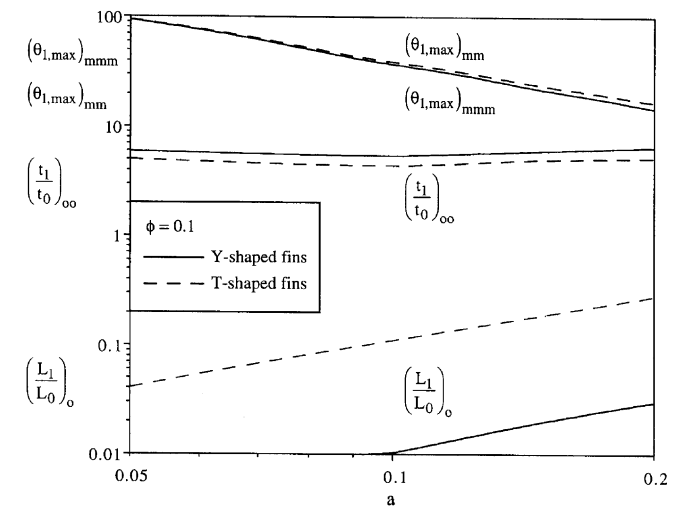


Fig. 10. Comparison of the general performances of T-shaped and Y-shaped fins.

the optimal ratio  $\left(\frac{L_1}{L_0}\right)_o$  is approximately ten times larger in the T-shaped fins than the Y-shaped fins.

## 6. Concluding remarks

This work showed numerically that the dimensionless global thermal resistance of the Y-shaped assembly of fins can be minimized by geometric optimization subject to total volume and fin material constraints. The triple optimization (Figs. 2–4) showed the emergence of an optimal external shape for the assembly,  $(L_1/L_0)_o$ , an internal optimal ratio of plate-fin thicknesses,  $(t_1/t_0)_{oo}$ , and an optimal angle,  $\alpha_{ooo}$ , that minimizes the global thermal resistance when the parameters  $(a, \phi)$  are fixed. Parametric study showed that the global thermal resistance decreases monotonically as  $\phi$  and  $a$  increases. The triple optimized optimal angle,  $\alpha_{ooo}$ , also decreases when the parameter  $a$  increases, but it increases when  $\phi$  increases. These results were correlated by the power law

$$(\theta_{1,\max})_{\text{mmm}} = 0.82a^{-1.33} \phi^{-0.33} \alpha_{ooo}^{-0.07}$$

Finally, the performance of Y-shaped assembly of fins was compared with the one presented by the T-shaped assembly of fins. The Y-shaped structure performs better than the T-shaped one. This better performance increases with the value of the parameter  $(a)$  and it is approximately 11% larger when  $a = 0.2$ . It was also noted that the Y-shaped assembly of fins presents its internal optimal ratio of plate-fin thicknesses,  $(t_1/t_0)_{oo}$ , approximately 12% larger than the T-shaped ones while the T-shaped assembly of fins has the optimal external shapes,  $\left(\frac{L_1}{L_0}\right)_o$ , ten times larger than the ones optimized in the Y-shaped structure.

## Acknowledgements

Prof. Giulio Lorenzini's work was sponsored by the Italian Ministry for Education, University and Research.

Prof. Luiz Rocha's work was sponsored by FAPERGS, Porto Alegre, RS, Brazil and CNPq, Brasília, DF, Brazil.

## References

- [1] A. Bejan, Constructal-theory network of conducting paths for cooling a heat generating volume, *Int. J. Heat Mass Transfer* 40 (1997) 799–816.
- [2] J.V.C. Vargas, J.C. Ordóñez, A. Bejan, Constructal PEM fuel cell stack design, *Int. J. Heat Mass Transfer* 48 (2005) 4410–4427.
- [3] A. Bejan, N. Dan, Two constructal routes to minimal heat flow resistance via greater internal complexity, *J. Heat Transfer* 121 (1999) 6–14.
- [4] L.A.O. Rocha, S. Lorente, A. Bejan, Constructal design for cooling a disc-shaped are by conduction, *Int. J. Heat Mass Transfer* 45 (8) (2003) 1642–1652.
- [5] A. Bejan, *Shape and Structure, from Engineering to Nature*, Cambridge University Press, Cambridge, UK, 2000.
- [6] A.D. Kraus, Developments in the analysis of finned arrays, Donald Q. Kern Award Lecture, National Heat Transfer Conference, Baltimore, MD, August 11, 1997, *Int. J. Transport Phenom.* 1 (1999) 141–164.
- [7] A. Aziz, Optimum dimensions of extended surfaces operating in a convective environment, *Appl. Mech. Rev.* 45 (5) (1992) 155–173.
- [8] J. Bonjour, L.A.O. Rocha, A. Bejan, F. Meunier, Dendritic fins optimization for a coaxial two-stream heat exchanger, *Int. J. Heat Mass Transfer* 47 (1) (2004) 111–124.
- [9] R.S. Matos, T.A. Laursen, J.V.C. Vargas, A. Bejan, Three-dimensional optimization of staggered finned circular and elliptic tubes in forced convection, *Int. J. Therm. Sci.* 43 (2004) 477–487.
- [10] C. Biserni, L.A.O. Rocha, A. Bejan, Inverted fins: geometric optimization of the intrusion into a conducting wall, *Int. J. Heat Mass Transfer, USA* 47 (12–13) (2004) 2577–2586.
- [11] L.A.O. Rocha, E. Lorenzini, C. Biserni, Geometric optimization of shapes on the basis of Bejan's constructal theory, *Int. Commun. Heat Mass Transfer* 32 (10) (2005) 1281–1288.
- [12] A. Bejan, M. Almgöbel, *Int. J. Heat Mass Transfer* 43 (2000) 2101–2115.
- [13] MATLAB, User's guide, version 6.0.088, release 12, The Mathworks Inc., 2000.